Formation of vortices in first order phase transitions

Alejandra Melfo*
International School for Advanced Studies (SISSA-ISAS), Strada Costiera 11, 34014 Trieste, Italy, and Laboratorio de Física Teórica, Facultad de Ciencias, Universidad de Los Andes, Mérida 5101-A, Venezuela

Leandros Perivolaropoulos†
Center for Theoretical Physics, Massachussets Institute of Technology, 77 Massachussetts Avenue, Cambridge, Massachussets 02139 and Department of Physics, Brown University, Providence, Rhode Island 02912

(Received 23 January 1995)

Using a toy model Lagrangian we investigate the formation of vortices in first order phase transitions. The evolution and interactions of vacuum bubbles are also studied using both analytical approximations and a numerical simulation of scalar field dynamics. A long-lived bubble wall bound state is discovered and its existence is justified by using a simplified potential for the bubble wall interaction. The conditions that need to be satisfied for vortex formation by bubble collisions are also studied with particular emphasis placed on geometrical considerations. These conditions are then implemented in a Monte Carlo simulation for the study of the probability of defect formation. It is shown that the probability of vortex formation by the collision of relativistically expanding bubbles gets reduced by about 10% due to the above-mentioned geometric effects.

PACS number(s): 11.27.+d, 11.15.Ex, 64.60.Qh, 98.80.Cq

I. INTRODUCTION

Symmetry-breaking phase transitions in the early Universe can give rise to topologically stable localized energy concentrations known as *topological defects* (for recent reviews see Refs. [1–3]). These defects can be points (monopoles), lines (cosmic strings), or surfaces (domain walls) depending on the homotopy of the vacuum manifold of the broken phase [4].

In general when a symmetry group G is spontaneously broken to a smaller group H, defects can form if the resulting vacuum manifold $M = G/H$ has nontrivial homotopy. Cosmic strings (vortices in two space dimensions) form when the first homotopy group of M is nontrivial: i.e., $\pi_1(M) \neq 1$.

Consider for example the Lagrangian density describing the dynamics of a complex scalar field $\Phi = \Phi_1 + i\Phi_2$:

$$\mathcal{L} = \frac{1}{2}\partial_\mu \Phi^* \partial^\mu \Phi - V(|\Phi|), \tag{1}$$

where $V(|\Phi|)$ is minimized for $|\Phi| = \sigma \neq 0$ [e.g., $V(\Phi) = \frac{\lambda}{4}(|\Phi|^2 - \sigma^2)^2$]. The set of potential minima of $V(|\Phi|)$ ($\Phi = \sigma e^{i\alpha}$) has the topology of a circle S^1. In a cosmological setup, according to the Kibble mechanism [5], there will be (by causality) field configurations that span the whole vacuum manifold as we go around a large circle in physical space (i.e., asymptotically $\Phi \to \sigma e^{i\theta}$ where θ is the azimuthal angle in physical space). Such configurations will inevitably form [6] (but see Ref. [7] for potential loopholes in the gauge case), with probability about $\frac{1}{4}$ [8], when causally disconnected domains of the Universe merge as the causal horizon expands. The asymptotic behavior $\Phi \to \sigma e^{i\theta}$ implies by continuity of Φ that there will be a point inside the large circle where $\Phi = 0$. This point (and its neighborhood) being outside of the vacuum manifold will be associated with topologically trapped energy density. This configuration is the topologically stable vortex [9]. Extended to three dimensions this object becomes a line defect, the *cosmic string.*

In the above-simplified Lagrangian (1) no gauge fields are involved and the broken symmetry is a U(1) global symmetry leading to the formation of *global vortices.* The price to pay for considering a simple U(1) global rather than a U(1) gauge symmetry [9] is that the total energy of an isolated global vortex diverges logarithmically. This however is not a problem in systems where a physical cutoff scale is built in, like multivortex systems where the cutoff scale is the intervortex separation, or cosmological setups where the cutoff is the horizon scale. For simplicity in what follows we will consider sytems with global rather than gauge symmetry breaking.

The above picture of string formation when regions of the size of the horizon at the phase transition become causally connected is characteristic of systems undergoing a second order phase transition ([10], see [11] for a recent discussion). In systems undergoing first order phase transitions, vortices can form by the merging of expanding vacuum bubbles with scalar field phases such that the whole vacuum manifold is covered after the bubble colli-

*Electronic address: melfo@galileo.sissa.it
†Electronic address: leandros@mitlns.mit.edu

sion and phase interpolation.[1] Consider, for example, an area ΔA of a two-dimensional system undergoing a first-order phase transition during a time interval ΔT. There are three basic conditions that need to be satisfied for a vortex to form within the area ΔA during the time ΔT: (1) The nucleation of at least three bubbles must take place during ΔT; (2) the nucleated bubbles must have phases such that geodesic interpolation leads to complete coverage of the vacuum manifold S^1; (3) the initial geometric configuration of the three nucleated bubbles must be such that the collision of all three bubbles occurs before the phase interpolation process can spoil the previous condition. Thus, the probability for a vortex to form within ΔA during the time interval ΔT may be written as

$$P_{\rm tot}(\Delta A, \Delta T) = B^3 P_{\rm phase}(B) S(B, v), \qquad (2)$$

where $B \equiv \Gamma \frac{\Delta A}{A_{\rm bub}} \Delta T$ is the probability for a true vacuum bubble of area $A_{\rm bub}$ to form within ΔA during time ΔT, $P_{\rm phase}(B)$ is the probability that a geodesic interpolation of the bubble phases completely covers the vacuum manifold. The dependence on the probability B exists because $P_{\rm phase}(B)$ is larger for clustered defects and therefore it increases with B. The suppression factor $S(B, v)$ depends on the bubble formation probability and the bubble wall expansion velocity v, and is the probability that the initial configuration of bubbles will be such that the third condition is satisfied.

The factor $P_{\rm phase}(B)$ has been calculated in previous studies and found to be between 0.25 and 0.31 depending on the number of clustered vortices. One of the main goals of this work is to find the suppression factor $S(B, v)$ for relativistically expanding bubbles ($v \simeq 1$). The case when bubbles expand in the presence of plasma [14] ($v < 1$) is significantly more complicated [16] and will be included in a separate publication [15].

In the next section we derive and solve numerically (and analytically in the thin bubble wall limit) the instanton equations for bubble formation. We use a simple scalar field potential with vacuum manifold S^1 describing a first order phase transition. The obtained scalar field configurations are then evolved by using a numerical simulation based on a second order accurate leapfrog algorithm [17]. We first focus on the bubble interactions and study their dependence on the phase difference between the two bubbles, both numerically and in the context of a simple analytic model. After justifying analytically the numerically observed existence of long-lived states of repelling walls in the limit of a large phase difference, we show that no metastable states exist in the model considered. Thus all colliding bubbles eventually merge and the existence of metastable embedded walls need not be a consideration for studying vortex formation. The formation of relativistic phase waves after bubble collisions is also seen in our simulations, confirming expectations from previous studies.

In Sec. III, we focus on the probability of vortex formation during three bubble collisions. We first briefly discuss the factor $P_{\rm phase}(B)$ and show how its dependence on the vacuum decay rate Γ, which has been ignored in most previous studies, can be used to explain previous numerical results [13] that seemed puzzling at the time of their derivation. We then focus on the geometric suppression factor $S(B, v \simeq 1)$ and first derive the geometrical conditions under which the vortex formation is suppressed. These conditions are then tested by using dynamical simulations of three bubble collisions, and a Monte Carlo simulation is constructed based on these conditions to obtain the dependence of the suppression factor S on the mean interbubble distance and therefore on the bubble formation probability B. Finally, in Sec. IV we conclude and briefly discuss extensions of this work that are currently in progress.

II. BUBBLE EVOLUTION AND INTERACTIONS

Consider a complex scalar field $\Phi = |\Phi| e^{i\alpha}$, in a (2+1)-dimensional spacetime, whose dynamics is determined by the Lagrangian (1) and a symmetry-breaking potential

$$V = \lambda \left[\frac{|\Phi|^2}{2} (|\Phi| - \sigma)^2 - \frac{\epsilon}{3} \sigma |\Phi|^3 \right] \qquad (3)$$

with $\epsilon \geq 0$ (Fig. 1).

The false vacuum ($\Phi = 0$) of the potential (3) decays via bubble nucleation to the true vacuuum ($|\Phi| = \sigma\eta \equiv \sigma \frac{1}{4}[3 + \epsilon + \sqrt{(3+\epsilon)^2 - 8}]$). The two-dimensional field configurations of the bubbles nucleated during this first order phase transition can be obtained [18] (see also [19]

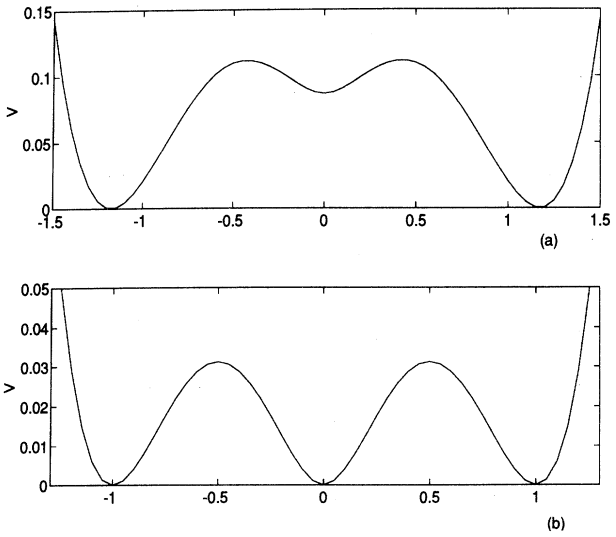

FIG. 1. The potential for (a) $\epsilon = 0.2$ and (b) $\epsilon = 0.0$, normalized at 0 at the true vacuum.

[1] Subcritical bubbles [12] can also play a minor role in vortex formation [13] but those effects are ignored within our approximation.

for a review) by solving the Euclidean field equations

$$\frac{\partial^2\Phi}{\partial\rho^2}+\frac{2}{\rho}\frac{\partial\Phi}{\partial\rho}=\frac{\partial V(|\Phi|)}{\partial|\Phi|} \tag{4}$$

with $\rho^2=|\vec{x}|^2+\tau^2$, τ being Euclidean time. The initial configuration of the field after tunneling has therefore an O(3) symmetry. This symmetry of the initial bubbles will become O(2+1) symmetry in Minkowski spacetime, where $\rho^2=|\vec{x}|^2-t^2$. Solutions satisfy the boundary conditions

$$\phi\to 0 \text{ as } \rho\to\infty \text{ and } \frac{\partial\phi}{\partial\rho}\to 0 \text{ as } \rho\to 0. \tag{5}$$

Analytic solutions to (4) can be found in the so-called thin-wall approximation, i.e., for $\epsilon\ll 1$, when the energy difference between the minima is much smaller than the height of the potential barrier. For the potential (3), the thin-wall solution is of the form [20]

$$|\Phi|=\frac{\sigma}{2}\left[1-\tanh\left(\frac{\sqrt{\lambda}\sigma}{2}(\rho-R_0)\right)\right], \tag{6}$$

where $R_0=1/(\sqrt{\lambda}\sigma\epsilon)$ is the bubble's initial radius, found by minimizing the total energy.

In the general, or thick-wall case, solutions to (4) with the boundary conditions (5) can be obtained numerically using a relaxation technique [17]. An arbitrary constant phase is then assigned in the interior of each bubble and the resulting configurations are evolved by solving the dynamical field equations

$$\ddot{\phi}-\nabla^2\phi=-\frac{\partial V}{\partial\phi}, \tag{7}$$

where the dimensionless variables

$$\phi=\Phi/\sigma\ ,\quad \vec{x}=\vec{\tilde{x}}\,m\ ,\quad \text{and } t=\tilde{t}\,m \tag{8}$$

with $m=\sqrt{\lambda}\sigma$, were used. For this part of the code, a second order leapfrog scheme [17] was implemented on a 400 × 400 lattice, using as a reference the algorithm of Ref. [6]. Energy was conserved in all simulations to within 5% for the evolution time scales.

Defining the bubble walls as $\rho=R_0$, we see that the O(3 + 1) symmetry forces the bubbles to expand, approaching the speed of light on a time scale determined by the initial radius R_0 ($|\vec{x}_{\rm bub}|^2=R_0^2+t^2$). Because of Lorentz contraction, thick-wall bubbles rapidly become thin-walled ones. As a consequence, interactions between bubbles occur almost always in the thin-wall regime, but we have kept thick-wall bubbles as initial conditions for our simulations for generality. For the figures presented, we have used $\epsilon=0.8$ unless specified otherwise.

It is evident from the simulations that the two-bubble interactions are strongly influenced by the difference between the field phases. Walls of bubbles with phase differences $\Delta\alpha\sim\pi$ tend to repel each other at short distances, thus delaying the time of merging of the walls. As bubbles approach, this causes the walls to separate and come in contact again, producing an oscillating false-vacuum wall, as can be seen in Fig. 2. This domain wall eventually decays, its lifetime depending on the phase difference. The effect is clearly observed when $\Delta\alpha\geq 0.9\pi$. For phase differences of $\Delta\alpha\simeq\pi$, we have found lifetimes of 10 [in the dimensionless units of Eq. (8)]. Points in the wall located in the line joining the bubble's center oscillate with a period $T\simeq 4$ ($\epsilon=0.8$). Notice that this oscillatory state occurs *before* the bubbles merge, and is not to be confused with the oscillations of the field's magnitude that occur during bubble merging and after the phase interpolation has occured, as reported in [21,22]. The origin of the effect in this case is the balance between the repulsive force originating from the phase dif-

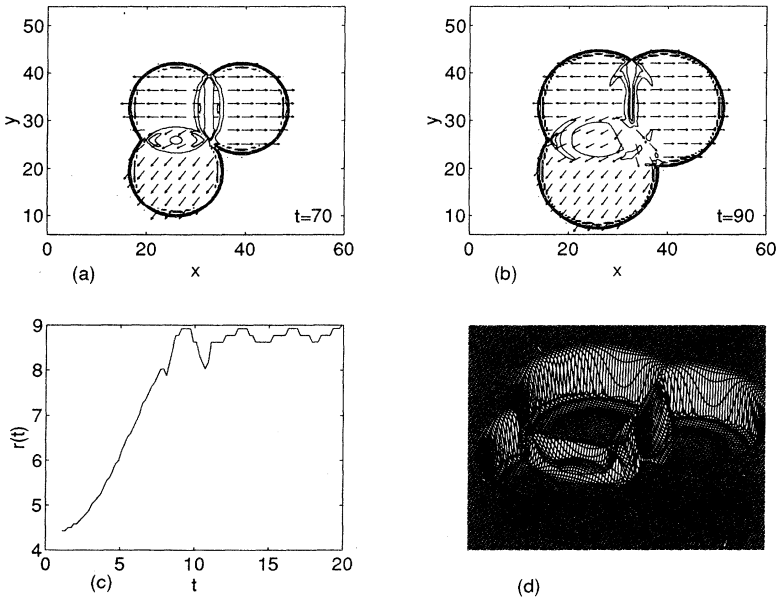

FIG. 2. Three-bubble interactions. Here and in the following figures the field's phase is indicated by the arrows, its magnitude by the contours and the size of the arrows. A metastable wall has been formed between the uppermost bubbles at $t=70$, in (a), and starts decaying at $t=90$, in (b). Phases are 1.3π, 0, and π, clockwise. In (c) plot the position of the wall of one bubble against time, in a two-bubble collision with opposite phases (differing by 0.9995π), showing the oscillating stage before merging. In (d) the field's magnitude is plotted, for the same geometry as (a) and (b), at $t=80$, showing the wall on one interface and the oscillations after merging in the other.

ference between colliding bubbles and the attractive force of the scalar field potential. On the other hand, in the oscillations discussed in Refs. [21,22] only the attractive potential force is relevant since the phase difference on opposite sides of the oscillating false vacuum is zero.

To better understand the numerically observed long-lived oscillating states we consider the problem in the planar approximation and write the equations of motion of bubble walls located at $x = \pm\xi(t)$ as

$$\sigma\ddot{\xi} = -\frac{\partial W}{\partial \xi}, \tag{9}$$

where σ is the mass per unit area of the wall, and W the static interaction energy between the walls, per unit area. Writing the field as $\phi = |\phi|e^{i\alpha}$, we have (primes denoting derivatives with respect to the spatial coordinate)

$$W = \int_{-\xi}^{\xi} dx \left[\frac{(|\phi|')^2}{2} + \frac{|\phi|^2(\alpha')^2}{2} + V(\phi)\right]. \tag{10}$$

As a first approximation, consider $V(\phi)$, $|\phi|$ and $|\phi|'$ as constants in the region between the bubble walls and $\alpha' = \Delta\alpha/2\xi$. The force between the walls will be

$$F \simeq -V(\bar{\phi}) - (|\bar{\phi}'|)^2 + \frac{|\bar{\phi}|^2(\Delta\alpha)^2}{4\xi^2}, \tag{11}$$

where $\bar{\phi}$ and $\bar{\phi}'$ are close but not exactly equal to zero. That is, the difference in phases produces a repulsive term dominating at short distances. This simple picture can be improved by considering the total field configuration as a sum of two bubble configurations, $\phi = |\phi|e^{i\alpha}$, with $|\phi|$ approximated by the sum of two thin-wall bubbles:

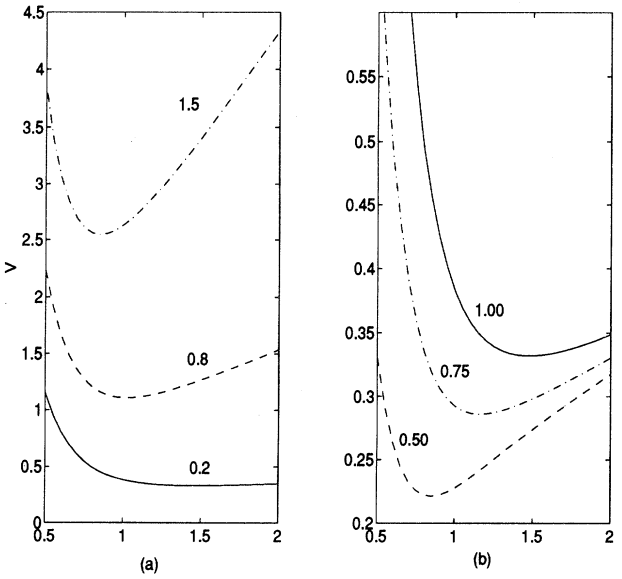

FIG. 3. The potential between two bubble walls as a function of the interbubble distance for (a) $\Delta\alpha = \pi$, and $\epsilon = 0.2$, 0.8, and 1.5, and (b) for $\epsilon = 0.2$ and $\Delta\alpha = \pi$, 0.75π, and 0.5π.

$$|\phi| = \frac{\eta}{2}\left[1 + \tanh\left(\frac{x-\xi}{2}\right)\right] + \frac{\eta}{2}\left[1 - \tanh\left(\frac{x+\xi}{2}\right)\right] \tag{12}$$

and $\alpha' = \Delta\alpha/2\xi$. The resulting potential energy W is plotted in Fig. 3 for different values of $\Delta\alpha$ and ϵ, as a function of ξ. Reducing ϵ has the effect of reducing the false vacuum potential energy, allowing the repulsive term to dominate at greater distances. The effect of increasing $\Delta\alpha$ is that of displacing the minimum of the potential to higher values of ξ. The approximation is expected to be valid only for $\xi \geq 1$, i.e., before the bubbles begin to merge. Our simulations have shown that the gradient is actually locally time dependent and the initially binding potential of Fig. 3 eventually gets dominated by the attractive terms as the phase gradient decreases locally.

The existence of these oscillatory states leads naturally to the question of existence of "embedded" metastable domain walls for this potential. Such domain walls would be static solutions to the field equations

$$|\phi|'' - (\alpha')^2|\phi| = \frac{\partial V}{\partial|\phi|},$$
$$\alpha'' + \frac{2}{|\phi|}|\phi|'\alpha' = 0, \tag{13}$$

with boundary conditions $\phi \to 0$ as $x \to 0$; $\phi \to \sigma\eta$ for $x \to \infty$. A simple asymptotic analysis suffices to prove that there is no solution to (13) satisfying the boundary conditions. As $x \to 0$, we can always write $|\phi| = C_\phi x^a$, $\alpha = C_\alpha x^b$. However, inserting this in (13) we obtain

$$a = \frac{1}{2}, \quad b = 0, \quad C_\alpha^2 = -\frac{1}{4}. \tag{14}$$

So the asymptotic form of the equations is not satisfied for a real coefficient C_α, and therefore the solution with the required boundary conditions does not exist. Thus the only possible domain wall occurs for $\Delta\alpha = \pi$, where the situation is analogous to that of a real field. Then Eqs. (13) become

$$|\phi|'' = \frac{\partial V}{\partial|\phi|} \tag{15}$$

with the boundary conditions $\phi = \pm\sigma\eta$ at $x \to \pm\infty$, and $\phi = 0$ at $x = 0$. The solutions are the domain walls in this potential. For ϵ nonzero, we can see that its existence is guaranteed by noting, as usual, that the problem is analogous to that of a particle moving in the potential $-V(\phi)$, with the field representing the particle's position and the spatial coordinate interpreted as a time coordinate. The "particle" is energetically allowed to start from $x = +\sigma\eta$ at $t = -\infty$, and arrive at $x = -\sigma\eta$ at $t = +\infty$. This is not the case when $\epsilon = 0$, and then only solitons that go from $x = \pm\sigma\eta$ to $x = 0$ are possible. But as we have seen, even in the case where this domain wall does exist, the asymptotic analysis above means that it is unstable under small variations of $\Delta\alpha$ (a static solution does not exist for $\Delta\alpha \neq \pi$). As discussed above this was

also verified by our simulations.

After the two bubbles merge, the situation is the one already studied numerically in [21] and analytically in [22]. A phase wave is generated in the contact point, and expands inside the bubbles with the speed of light, interpolating between the original phases. The field magnitude oscillates in the region of contact, with amplitude that depends in the phase difference, this time being inversely proportional: a greater phase difference will result in a more energetic phase wave, that carries away the wall's energy more efficiently thus dissipating the vacuum oscillations rapidly. These oscillations however do not affect the phase interpolation: the phase waves are produced as soon as the interiors of the bubbles come into contact, and escape at light speed.

III. VORTEX FORMATION

We turn now to discuss the probability of vortex formation in a three-bubble collision. As noted in the Introduction, the probability of forming three bubbles in an area ΔA within a period of time ΔT is B^3. In order to form a vortex, the phase of these three bubbles must be distributed so that the interpolation following collision leads to complete coverage of the vacuum manifold [condition (2)]. The probability for this to happen can be estimated as follows [8]: Consider a triangular lattice in a two-dimensional (2D) physical space and assign a random phase to each point on the lattice. The question is the following: *What is the probability that a vortex lies within a given triangle?* The mean phase difference of two neighboring lattice points of a triangle is clearly $2\pi/4$. In order that a vortex forms in that triangle, the whole vacuum manifold must be covered by interpolating the phases of the three lattice points and therefore the phase of the third lattice point of the triangle must lie on the opposite part of the phase circle. Thus, on the average, the phase of the third lattice point should be in a range of $2\pi/4$. This will happen with probability $P_v = 1/4$. Thus, the probability for forming an isolated vortex in physical space is $1/4$. In realistic cases however vortices do not form isolated but in vortex antivortex clusters especially when the vacuum decay rate is high. A very relevant question therefore is the following: *What is the probability for forming a vortex in a vortex antivortex cluster?* The probability p_{+-} for forming an antivortex next to an already formed vortex is larger than the probability for forming an isolated vortex. The reason is that the mean phase difference between neighboring lattice points in a vortex surrounding triangle is not $2\pi/4$ but $2\pi/3$ and therefore to form an antivortex next to a vortex we only need that the fourth lattice point be in a phase range $2\pi/3$. So $p_{+-} = 1/3$. Thus, the probability for having i antivortices around a vortex is

$$P_i = \binom{3}{i} (P_{+-})^i (1 - P_{+-})^{3-i} \qquad (16)$$

and the probability per defect in clusters of four or larger is $(P_{+-}^3 P_v)^{1/4} = 0.31$ which is significantly larger than the naively obtained result of 0.25.

This effect of clustering explains the result found in Ref. [13], where a simulation of the vortex formation process is done by placing random-phase bubbles in a two-dimensional lattice, and allowing them to evolve and collide. The author finds a probability of vortex and antivortex formation of 0.42 (10 vortices and antivortices formed after the nucleation of 23 closely packed bubbles), instead of the expected 0.25, and attributes his result to unknown dynamical effects. However, if we notice that the chosen rate of nucleation produces a highly packed system, and calculate the probability using (16), we obtain a higher value.

The dynamical delay of merging due to the phase repulsive potential, discussed in the previous section, does not affect vortex formation. The phase interpolation will occur eventually, and the crucial factor is not the time it takes, but the spatial range over which the bubbles overlap, which determines the spatial sectors where phases will interpolate. A phase repulsion [which in any case occurs for $\Delta\alpha$ extremely close to π, an unlikely situation if the phases are required to be distributed in the vacuum manifold as in condition (1) of the Introduction], can only delay the interpolation event. In the formation of vortices, it is only important to know *if* (not *when*) the phases of each of the three bubble pairs will geodesically interpolate.

In addition, for the case of bubbles with relativistic velocities (i.e., when the effects of the plasma are negligible), we have both the bubble walls and the phases propagating at $v \simeq 1$. This means that the phase waves can never reach the bubble walls leading to a single new bubble with interpolated phase, before the third bubble has time to reach the two collided ones.

Thus, in the absence of plasma, the important ingredient needed to find the probability of vortex formation is the initial geometric distribution and nucleation times

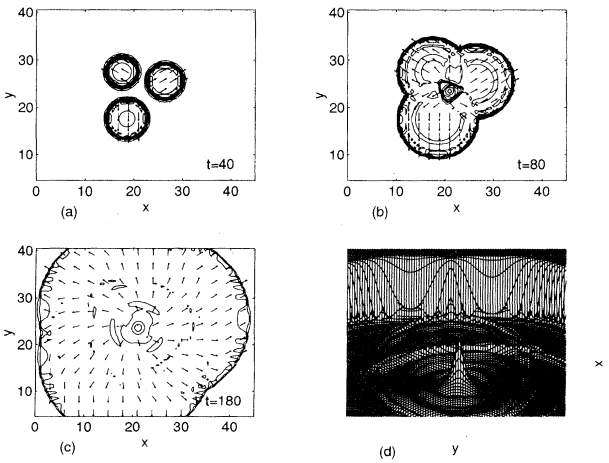

FIG. 4. Three-bubble collision. (a)–(c) are a sequence of a three-bubble collision for $t = 40$, 80, and 180 as indicated, showing the formation of the vortex. The magnitude of the field is plotted in (d), for $t = 170$, showing the newly formed vortex.

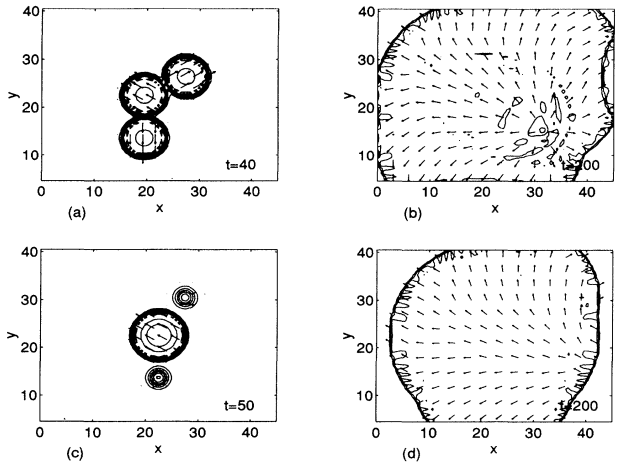

FIG. 5. Three-bubble collisions. In (a) and (b), bubbles nucleate simultaneously at the vertices of an obtuse triangle, producing a vortex. In (c) and (d), bubbles nucleate at different times in a nonaligned configuration, with the same phase distribution as above, but the difference in sizes prevents the circles to intersect, thus the vortex is not formed.

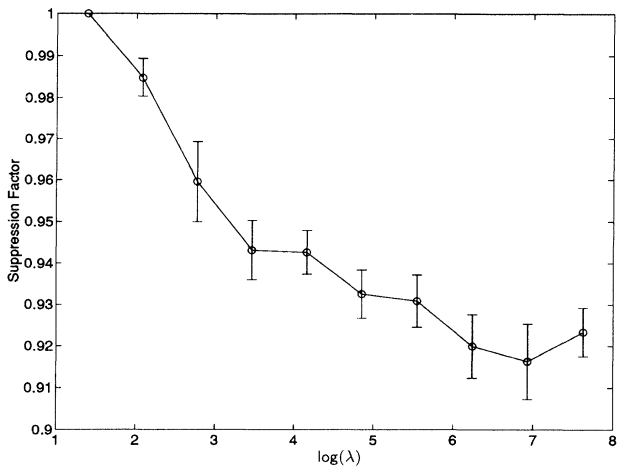

FIG. 6. Suppression factor $S(B)$ as a function of λ. The logarithm is to base e.

of the colliding bubbles. In the case when the effects of plasma are ignored ($v \simeq 1$) simulations show (Fig. 4) that we can picture the bubbles as circles, even when the merging has occurred, the phase wave front continuing the circle formed by the walls.

For a vortex to form, then, it is easy to see that condition (3) of Sec. I is satisfied *if the three expanding circles have at least one common intersection point.* Thus, for example, the extreme case of three bubbles of the same size (i.e., nucleated at the same time), but with centers located along a straight line, will not form a vortex. If we allow for different nucleation times, bubbles will interact having different sizes, and then even nonaligned configurations will not lead to a vortex (Fig. 5). Notice that in contrast with what has been stated in previous studies [22] it is in general not possible to select a frame where all bubbles nucleate at the same time. The condition of simultaneity of three events is that there is a *spacelike* planar surface that goes through these events. This is not always possible (consider for example the special case of three events on a straight line, i.e., effectively in one spatial dimension). Even if it was possible to select a frame of simultaneity for three events in $2+1$ dimensions it would not be appropriate to do so in a Monte Carlo simulation as this artificial selection of a frame would introduce a bias in the measured probabilities. We therefore have used different times for the nucleation of each bubble.

The equation of motion for the bubble walls is dictated by the initial configuration, as stated in the previous section, so that the radius of a bubble nucleated at time $t = \Delta t_i$ will be $r_i(t)^2 = R_0^2 + (t - \Delta t_i)^2$, the subindex i going from 1 to 3. Given the positions (x_i, y_i) and nucleation times of three bubbles, one has only to solve the system of three equations for the intersection point and time:

$$(x - x_i)^2 + (y - y_i)^2 = R_0^2 + (t - \Delta t_i)^2. \qquad (17)$$

A vortex forms if the solution to the system is real, positive and finite.

As a test for this condition, we have checked using the numerical simulation described in Sec. II the formation of vortices and predicted formation times for several configurations. The geometrical condition of a circle intersection was found to be accurate in all cases, confirming the hypothesis that dynamical effects can be ignored in the case of relativistically expanding bubbles.

Having tested the geometric model with dynamical simulations, a suppression factor for vortex formation can now be found using a Monte Carlo simulation. Random position and nucleation times were assigned for bubbles inside an area $\Delta A \equiv (\lambda R_0/2)^2$ and configurations were subject to the requirement that bubbles do not form in an overlapping state. After rescaling the considered area such that $R_0 = 1$, we constructed 500 randomly chosen three-bubble geometrical configurations. The system (17) was solved in each case and the number of cases with no triple intersection was counted. We defined the ratio of the number of cases where triple intersection occured over the total number of cases as the *suppression factor* for vortex formation. This is the factor $S(B, v \simeq 1)$ of Eq. (2). A plot of S vs $\lambda \sim B$ is shown in Fig. 6. Clearly the geometric suppression factor is less important for high nucleation rate (small λ) but it is not negligible for low nucleation rates.

IV. CONCLUSION

We have studied the basic conditions that are needed for vortex formation by the merging of vacuum bubbles nucleated during first order phase transitions. There are three such conditions which include the existence of three colliding vacuum bubbles, the complete coverage of the

vacuum manifold by geodesic interpolation of the bubble phases, and the existence of a triple collision point for the merging of the three circles that describe the relativistic expansion of the bubbles. The probability that each condition is satisfied was obtained and the result was compared with previous studies. In particular the existence of a triple collision point during the evolution of three colliding bubbles occurs with probability approximately 92% for low vacuum decay rate. Such a suppression of defect formation rate is not expected to modify in any major way cosmological models based on cosmic strings.

We have considered the case of relativistically expanding bubbles and have therefore neglected the friction effects of plasma particles surrounding the expanding vacuum bubbles. Such particles, being massless in the false vacuum but massive in the true vacuum (inside the bubble), are expected to scatter on the bubble walls and decelerate them to nonrelativistic velocities. In models where the effects of plasma are important enough to lead to slowly expanding bubbles, our analysis gives only an upper bound to the geometric suppression factor $S(B, v)$ which is expected to rapidly drop as the bubble wall velocity v decreases. Indeed, for small bubble wall velocity v, the interpolating phase front propagating *always relativistically* inside the bubbles after the first collision is more efficient in equilibrating the phases to the interpolated value before the third bubble reaches the bubbles that collided first. Thus the formation of the vortex can be avoided much more efficiently. The study of the dependence of S on v in the presence of plasma requires the detailed numerical simulation of the effects of the plasma, and the construction of a generalized geometrical model and Monte Carlo simulation based on these effects. That work is currently in progress [15].

ACKNOWLEDGMENTS

We would like to thank Tanmay Vachaspati and Alex Vilenkin for interesting discussions. We also thank Andrew Sornborger for his help with the numerics. Special thanks are due to Robert Brandenberger for insightful comments and discussion and for helping to make this collaboration possible. Finally one of us (A.M.) is grateful to the Physics Department of Brown University and SISSA-ISAS for financial support. The numerical part of this project was completed at the Center for Scientific Computing of Brown University. Financial support for this project was provided in part by DOE Grant Nos. DE-FG0291ER40688, Task A and DE-FC02-94ER40818.

[1] M.B. Hindmarsh and T.W.B. Kibble, "Cosmic Strings", Report No. SUSX-TP-94-74, 1994 (unpublished), p. 139 (bulletin board: hep-ph@xxx.lanl.gov-9411342).
[2] L. Perivolaropoulos, Contributed to Summer School in High Energy Physics and Cosmology, Trieste, Italy, 1994 (unpublished).
[3] R. Brandenberger, Int. J. Mod. Phys. A **9**, 2117 (1994).
[4] See, e.g., R. Rajaraman, *Solitons and Instantons* (North-Holland, Amsterdam, 1987), p. 78, and references therein.
[5] T.W.B. Kibble, J. Phys. **A 9**, 1387 (1976).
[6] J. Ye and R. Brandenberger, Mod. Phys. Lett. A **5**, 157 (1990); Nucl. Phys. **B346**, 149 (1990).
[7] S. Rudaz and A.M. Srivastava, Mod. Phys. Lett. A **8** 1443 (1993).
[8] R. Leese and T. Prokopec, Phys. Lett. B **260**, 27 (1991).
[9] H.B. Nielsen and P. Olesen, Nucl. Phys. **B61**, 45 (1973).
[10] T. Vachaspati and A. Vilenkin, Phys. Rev. D **30**, 2036 (1984); T. Vachaspati, *ibid.* **44**, 3723 (1991).
[11] R. Brandenberger and A. Davis, Phys. Lett. B **332**, 305 (1994).
[12] G. Gelmini and M. Gleiser, Nucl. Phys. **B419**, 129 (1994).
[13] A.M. Srivastava, Phys. Rev. D **46**, 1353 (1992).
[14] N. Turok, Phys. Rev. Lett. **68**, 1803 (1992); Bao-Hua Liu, Larry McLerran, and Neil Turok, Phys. Rev. D **46**, 2668 (1992); M. Dine, R. Leigh, P. Huet, A. Linde, and D. Linde, *ibid.* **46**, 550 (1992).
[15] A. Melfo and L. Perivolaropoulos (in preparation).
[16] T.W.B. Kibble (unpublished).
[17] W.H. Press *et al.*, *Numerical Recipes in FORTRAN: The Art of Scientific Computing*, 2nd ed. (Cambridge University Press, Cambridge, 1992).
[18] S. Coleman, Phys. Rev. D **15**, 2929 (1977).
[19] R. Brandenberger, Rev. Mod. Phys. **57**, 1 (1985).
[20] A.D. Linde, Nucl. Phys. **B216**, 421 (1983); **B223**, 544(E) (1983); *Particle Physics and Inflationary Cosmology* (Harwood Academic Publishers, Chur, 1990).
[21] S.W. Hawking, I.G. Moss, and J.M. Stewart, Phys. Rev. D **26**, 2681 (1982).
[22] M. Hindmarsh, A.C. Davis, and R. Brandenberger, Phys. Rev. D **49**, 1944 (1994).

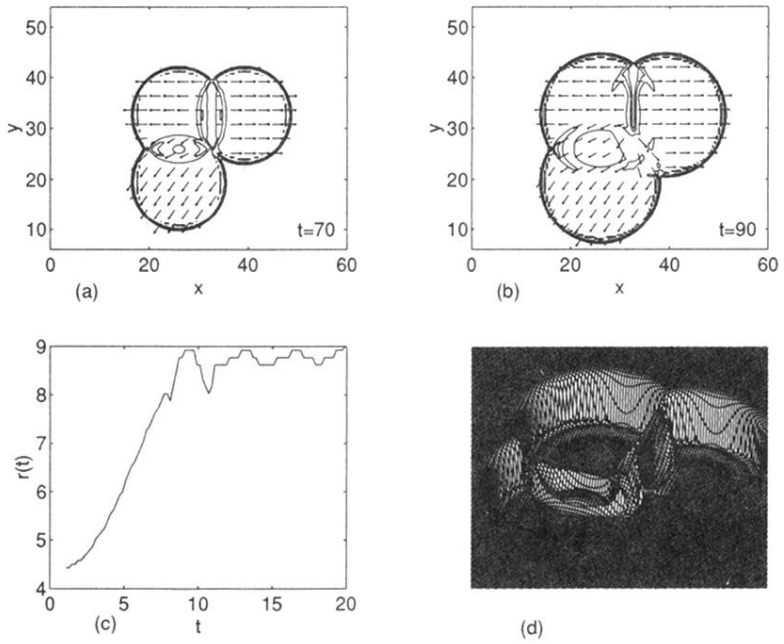

FIG. 2. Three-bubble interactions. Here and in the following figures the field's phase is indicated by the arrows, its magnitude by the contours and the size of the arrows. A metastable wall has been formed between the uppermost bubbles at $t = 70$, in (a), and starts decaying at $t = 90$, in (b). Phases are 1.3π, 0, and π, clockwise. In (c) plot the position of the wall of one bubble against time, in a two-bubble collision with opposite phases (differing by 0.9995π), showing the oscillating stage before merging. In (d) the field's magnitude is plotted, for the same geometry as (a) and (b), at $t = 80$, showing the wall on one interface and the oscillations after merging in the other.

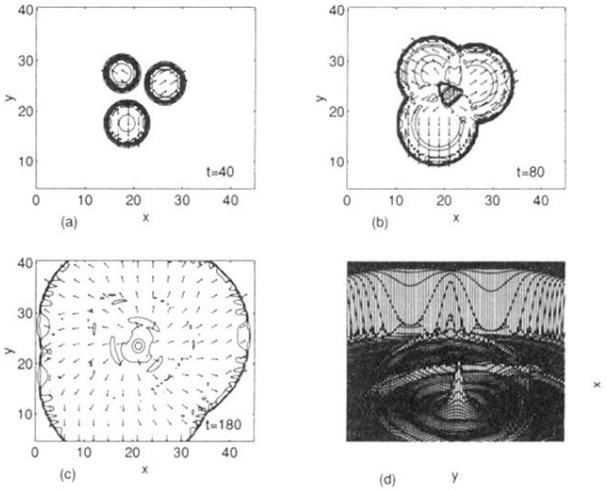

FIG. 4. Three-bubble collision. (a)–(c) are a sequence of a three-bubble collision for $t = 40$, 80, and 180 as indicated, showing the formation of the vortex. The magnitude of the field is plotted in (d), for $t = 170$, showing the newly formed vortex.